

Prompt Particle Acceleration to Relativistic Energies During Current Loop Coalescence in Solar Flares

Tohru Nakano* and Jun-ichi Sakai**

ABSTRACT

High energy particle acceleration during the current loop coalescence in solar flares is investigated by numerical simulation, based on the theoretical model derived by Sakai and Tajima (1986). Simulation results show that during the current loop coalescence, both electrons and protons can be quasi-periodically accelerated to relativistic energies within very short time ($\ll 1$ s). These results can give a good explanation for the prompt high energy particle acceleration during the impulsive phase of solar flares.

1. INTRODUCTION

The solar flare¹ is the explosive release process of magnetic energy stored in corona plasma. After launching of the Solar Maximum Mission (SMM)² and Hinotori satellites³, in particular, from the observations of solar flares with hard X-rays and γ -rays, it became⁴ clear that, within a second, protons and electrons are accelerated up to \sim GeV, up to \sim 100 MeV, respectively. They are beyond rest-mass energy. It seems difficult that these observational results can be explained by the former statistical acceleration mechanism like the Fermi-acceleration, which is slow acceleration process. Since the corona plasma flows along the magnetic flux tube which makes closed loop on the surface, many plasma current loops are observed in the flare region. Consequently, the reciprocal actions among these plasma current loops as well as magnetic flux tubes may be a very important role for the energy release process in solar flares. One of fundamental reciprocal action is the coalescence process^{5,6} of the two parallel plasma current loops, which currents flow in the same direction each other. In the coalescence process, under some conditions, magnetic energies of both current loops can be transformed to the kinetic energy of the whole plasma current through the explosive magnetic reconnection.^{7,8} At the same time, protons and electrons are accelerated rapidly to the relativistic energies. This phenomenon has been already shown by simulation and theory (current loop coalescence model)^{9,10}.

In this paper, we will report the detailed simulation results, using the theoretical coalescence model,¹¹ and show that both electrons and protons can be promptly accelerated to relativistic

*Department of Electronics Engineering

**Department of Applied Mathematics and Physics, Faculty of Engineering, Toyama University, Toyama 930 JAPAN

tic energies during the current loop coalescence.

In section 2 we review the theoretical model of the current loop coalescence and derive basic equations.

In section 3 we discuss the normalized basic equations, initial values and parameters for computations.

In section 4 we present the numerical results.

In section 5 we summarize our results.

2. THEORETICAL MODEL OF THE COALESCENCE PROCESS

In this section we review the theoretical model^{10,11} of current loop coalescence process, and derive the basic equations.

2.1 Definition of Theoretical Model

This model is treated in rectangular coordinate system, where x is the direction of coalescence, while y is the direction of poloidal magnetic field line and z is the direction of plasma current (See Fig.1). And we assume that $\partial/\partial x \gg \partial/\partial y, \partial/\partial z$. This means that every quantity is dependent only on x and time. Therefore, it is treated as one-dimensional problem. The basic equations we start are the two-fluid model equations of plasma and the Maxwell equations. They read as follows,

$$\frac{\partial}{\partial t} n_j + \nabla \cdot (n_j \mathbf{V}_j) = 0, \quad (2.1)$$

$$m_j n_j \frac{d}{dt} \mathbf{V}_j = n_j e_j \left(\mathbf{E} + \frac{\mathbf{V}_j}{c} \times \mathbf{B} \right) - \nabla p_j, \quad (2.2)$$

$$\nabla \times \mathbf{B} = \frac{4\pi}{c} \sum_j n_j e_j \mathbf{V}_j, \quad (2.3)$$

$$\nabla \cdot \mathbf{E} = 4\pi \sum_j n_j e_j, \quad (2.4)$$

$$\nabla \times \mathbf{E} = -\frac{1}{c} \frac{\partial}{\partial t} \mathbf{B}, \quad (2.5)$$

$$\frac{\partial}{\partial t} p_j + \mathbf{V}_j \cdot \nabla p_j + \gamma p_j \nabla \cdot \mathbf{V}_j = 0, \quad (2.6)$$

where j denotes the species of particles (proton or electron) and γ is the ratio of heat capacity which is related to the degree of freedom of the system f as $\gamma = 1 + 2/f$.

Here we neglected the displacement current in Eq. (2.3), because the flow speed during the current loop coalescence is slow compared with the light velocity. In the coalescence process, the scale-length involved in the system is not constant but varies continuously in time. Therefore the system can keep its global structure without changing whole structure of current loops, even if every quantity varies with time.

Such a physical situation may be described by self-similar solutions in which scale factors vary continuously. We introduce two scale factors $a(t)$ and $b(t)$ for both proton and electron flow velocities as follows,

$$V_{ex} = \frac{\dot{a}}{a}x, \tag{2.7}$$

$$V_{ix} = \frac{\dot{b}}{b}x, \tag{2.8}$$

where a dot represents the time derivative. The linear dependence on x for velocities implies that protons and electrons stream in opposite direction around the center of current sheet ($x=0$). These scale factors $a(t)$ and $b(t)$ will be self-consistently determined from the above basic equations. Now, we derive the equations of various quantities, related to the coalescence process.

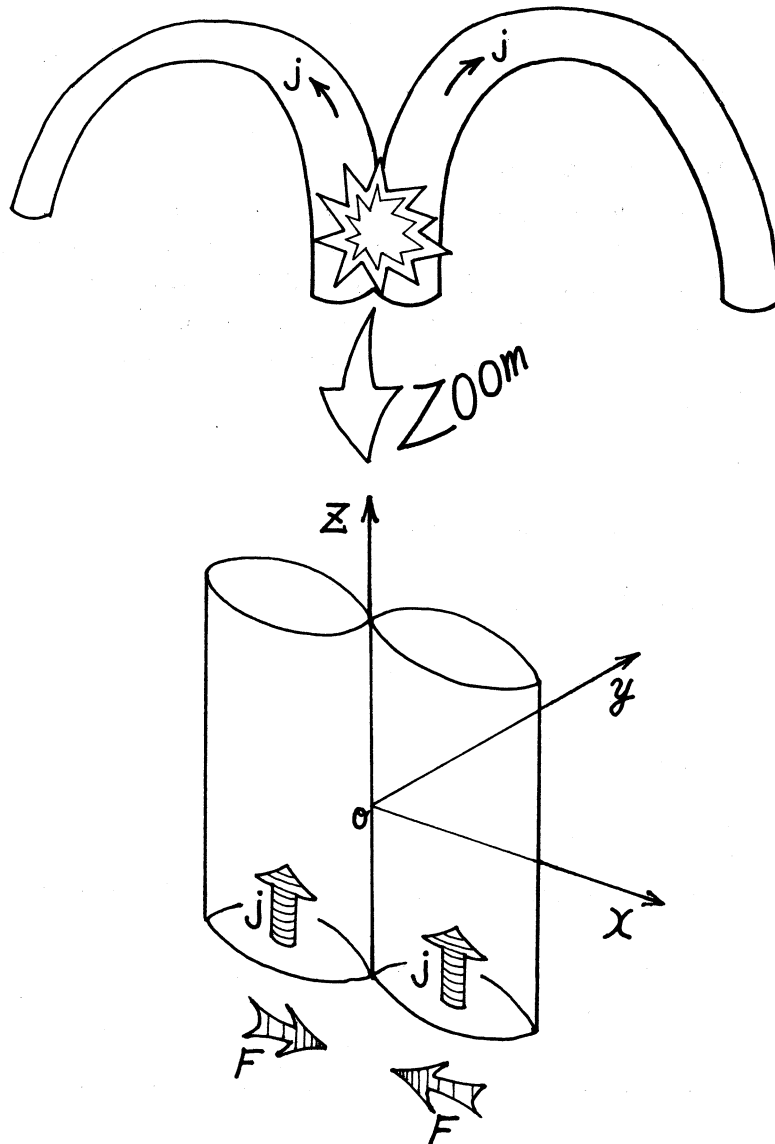


Fig.1. Coordinate system and schematic picture showing loop-loop coalescence: j is current density and F is attraction force.

2.2 Derivation of Particle Density n

The continuity equation of particles, Eq. (2.1), becomes a simpler expression as follows, because of one-dimensional problem, $\partial/\partial y \equiv 0$, $\partial/\partial z \equiv 0$.

$$\frac{\partial}{\partial t} n_j + n_j \frac{\partial}{\partial x} V_{jx} = 0 \quad (2.1)'$$

where we assumed that the density n_j depends only on time. This assumption is consistent with Eqs. (2.7) and (2.8). For electrons, We have from Eq. (2.7)

$$\frac{\partial}{\partial x} V_{ex} = \frac{\dot{a}}{a}.$$

Substituting above equation into Eq. (2.1)', we obtain

$$\frac{\dot{n}_e}{n_e} + \frac{\dot{a}}{a} = 0.$$

Integrating the both sides of the above equation by time, we obtain

$$n_e = \frac{n_0}{a}. \quad (2.9)$$

For protons, we have in a similar manner

$$n_i = \frac{n_0}{b}. \quad (2.10)$$

2.3 Derivation of Magnetic Field B

We assume that $B_x = 0$, and $B_z = \text{constant}$ in this model. So, we derive only the y -component B_y .

At first, from the y -component of Eq. (2.5) we obtain

$$\frac{\partial}{\partial z} E_x - \frac{\partial}{\partial x} E_z = -\frac{1}{c} \frac{\partial}{\partial t} B_y. \quad (2.5)'$$

Assuming that B_y varies like $B_y = B_0(t) \cdot x/\lambda$, we get

$$\frac{\partial}{\partial t} B_y = \dot{B}_0 \frac{x}{\lambda}.$$

Substituting this into Eq. (2.5)' (note $\partial E_x/\partial z = 0$),

$$\frac{\partial}{\partial x} E_z = \frac{x}{c\lambda} \dot{B}_0. \quad (2.5)''$$

Furthermore, we assume $E_x = E_{z0}(t) + E_{z1}(t) \cdot x^2/\lambda^2$ and differentiate both sides by x . Then we have

$$\frac{\partial}{\partial x} E_z = E_{z1}(t) \cdot \frac{2x}{\lambda^2}.$$

Substituting this into Eq. (2.5)'', we obtain

$$E_{z1}(t) = \frac{\lambda}{2c} \dot{B}_0. \quad (2.11)$$

From the z -component of Eq. (2.2), we have

$$m_j \frac{d}{dt} V_{jz} = e_j \left[E_z + \frac{1}{c} \cdot (V_{jx} B_y - V_{jy} B_x) \right].$$

Assuming $a(t) = b(t)$ and substituting $E_z = E_{z0}(t) + E_{z1}(t) \cdot x^2/\lambda^2$, $B_x = 0$, $B_y = B_0(t) \cdot x/\lambda$,

$\partial V_{jz}/\partial z = 0$, and Eq.(2.7) into above equation, we obtain

$$m_j \frac{\partial}{\partial t} V_{jz} = e_j \left[E_{z0}(t) + E_{z1}(t) \cdot x^2/\lambda^2 + \frac{\dot{a}}{a} \cdot \frac{B_0(t)}{\lambda c} \cdot x^2 \right].$$

This equation can be re-written as

$$m_j \frac{\partial}{\partial t} V_{jz} - e_j E_{z0}(t) = \frac{e_j}{\lambda} \left[\frac{E_{z1}(t)}{\lambda} + \frac{\dot{a}}{a} \cdot \frac{B_0(t)}{c} \right] x^2.$$

To satisfy this equation on any x value, both sides must be zero. Hence, we get

$$m_j \frac{\partial}{\partial t} V_{jz} - e_j E_{z0}(t) = 0, \quad (2.12)$$

$$\frac{E_{z1}(t)}{\lambda} + \frac{\dot{a}}{a} \cdot \frac{B_0(t)}{c} = 0. \quad (2.13)$$

From Eqs.(2.11) and (2.13), we have

$$\frac{\dot{B}_0}{B_0} = -2 \cdot \frac{\dot{a}}{a},$$

which gives by integrating both sides,

$$B_0(t) = \frac{B_{00}}{a^2}, \quad (2.14)$$

where B_{00} is a constant.

Thus, we obtain

$$B_y = \frac{B_{00}}{a^2} \cdot \frac{x}{\lambda}. \quad (2.15)$$

2.4 Derivation of Electric Field E

We assume $E_y = 0$ in this model. So, we derive the x and z -component of **E**.

2.4.1 DERIVATION OF x -COMPONENT E_x

From the Poisson's equation (2.4),

$$\frac{\partial}{\partial x} E_x + \frac{\partial}{\partial y} E_y + \frac{\partial}{\partial z} E_z = 4\pi e \cdot (n_i - n_e).$$

Substituting Eqs.(2.9) and (2.10) into this equation, (note: $\partial/\partial y \equiv 0$ and $\partial/\partial z \equiv 0$)

$$\frac{\partial}{\partial x} E_x = 4\pi e n_0 \cdot \left[\frac{1}{b} - \frac{1}{a} \right].$$

Assuming E_x as $E_x = E_0(t) \cdot x/\lambda$, we obtain for $E_0(t)$

$$E_0(t) = 4\pi e n_0 \lambda \cdot \left[\frac{1}{b} - \frac{1}{a} \right].$$

Therefore, we have

$$E_x = 4\pi e n_0 x \cdot \left[\frac{1}{b} - \frac{1}{a} \right]. \quad (2.16)$$

In this way, E_x has been derived, and we try to represent E_x without $b(t)$.

From the z -component of Eq.(2.3),

$$\frac{\partial}{\partial x} B_y - \frac{\partial}{\partial y} B_x = \frac{4\pi e}{c} \cdot (n_i V_{iz} - n_e V_{ez}).$$

Substituting $B_x = 0$, $B_y = B_0(t) \cdot x / \lambda$, and Eqs. (2.9), (2.10) into the above equation, we obtain

$$\frac{B_0(t)}{\lambda} = \frac{4\pi en_0}{c} \cdot \left[\frac{V_{iz}}{b} - \frac{V_{ez}}{a} \right]. \quad (2.17)$$

From Eq. (2.12), we have the two expressions for protons and electrons as follows,

$$m_i \cdot \frac{\partial}{\partial t} V_{iz} = eE_{z0}(t), \quad m_e \cdot \frac{\partial}{\partial t} V_{ez} = -eE_{z0}(t). \quad (2.18)$$

Eliminating $E_{z0}(t)$ from (2.18), we obtain

$$m_e \cdot \frac{\partial}{\partial t} V_{ez} = -m_i \cdot \frac{\partial}{\partial t} V_{iz}.$$

Integration both sides by time gives

$$m_e \int dV_{ez} = -m_i \int dV_{iz}.$$

Hence we get

$$V_{iz} = -\frac{m_e}{m_i} \cdot V_{ez}. \quad (2.19)$$

From Eqs. (2.17) and (2.19), we obtain

$$\frac{B_0(t)}{\lambda} = -\frac{4\pi en_0}{c} \cdot \left[\frac{m_e}{m_i} \cdot \frac{1}{b} + \frac{1}{a} \right] \cdot V_{ez}.$$

Substituting Eq. (2.14) into this, we obtain for V_{ez}

$$V_{ez} = -\frac{cB_{00}b}{4\pi en_0 \lambda a^2 \cdot \left[\frac{b}{a} + \frac{m_e}{m_i} \right]}.$$

Neglecting the mass ratio ($m_e/m_i \approx 0$), we obtain

$$V_{ez} = -\frac{cB_{00}}{4\pi en_0 \lambda a}. \quad (2.20)$$

Furthermore, the x -component of Eq. (2.2) becomes

$$m_e n_e \frac{d}{dt} V_{ex} = n_e e e_e \cdot \left[E_x + \frac{V_{ey} B_z - V_{ez} B_y}{c} \right] - \frac{\partial}{\partial x} p_e. \quad (2.21)$$

Here, we define p_e as follows,

$$p_e = \frac{p_{0e}}{a^\gamma} - \frac{p_{0e}}{2a^{\gamma+2}} \cdot \frac{x^2}{\lambda^2},$$

where p_{0e} is a constant.

Then, we obtain

$$\frac{\partial}{\partial x} p_e = -\frac{p_{0e}}{a^{\gamma+2}} \cdot \frac{x}{\lambda^2} \quad (2.22)$$

And we obtain by use of Eq. (2.7)

$$\frac{d}{dt} V_{ex} = \frac{\ddot{a}}{a} \cdot x \quad (2.23)$$

Substituting Eqs. (2.15), (2.16), (2.20), (2.22), and (2.23) into (2.21), we obtain

$$\ddot{a} = -\omega_{pe}^2 \cdot \left[\frac{a}{b} - 1 \right] - \frac{B_{00}^2}{4\pi m_e n_0 \lambda^2 a^2} + \frac{p_{0e}}{m_e n_0 \lambda^2 a^\gamma} \quad (2.24)$$

where $\omega_{pe}^2 = 4\pi e^2 n_0 / m_e$.

If we define p_i and ω_{pi}^2 for protons as follows,

$$p_i = \frac{p_{0i}}{b} - \frac{p_{0i}}{2b} \frac{x^2}{\lambda^2}, \quad \omega_{pi}^2 = \frac{4\pi e^2 n_0}{m_i}.$$

We can obtain the following equation for protons:

$$\ddot{b} = \omega_{pi}^2 \cdot \left[1 - \frac{b}{a} \right] + \frac{p_{0i}}{m_i n_0 \lambda^2 b} \quad (2.25)$$

If we define the Alfvén velocity V_a as

$$V_a^2 = \frac{B_{00}^2}{4\pi n_0 (m_i + m_e)} \approx \frac{B_{00}^2}{4\pi n_0 m_i} \quad (m_e/m_i \approx 0),$$

Then we obtain from Eq.(2.24)

$$\frac{1}{b} - \frac{1}{a} = \left[-\frac{m_i V_a^2}{\lambda^2 a^3} + \frac{p_{0e}}{n_0 \lambda^2 a^{\gamma+1}} \right] / (4\pi n_0 e^2).$$

Substituting this into Eq.(2.16), we finally obtain

$$E_x = \left[-\frac{m_i V_a^2}{e \lambda a^3} + \frac{p_{0e}}{e \lambda a^{\gamma+1} n_0} \right] \cdot \frac{x}{\lambda}. \quad (2.26)$$

2.4.2 DERIVATION OF z -COMPONENT E_z

Since $E_z = E_{z0}(t) + E_{z1}(t) \cdot x^2 / \lambda^2$, we eliminate $E_{z0}(t)$ and $E_{z1}(t)$ from it, using Eqs.(2.12) and (2.13). Then we have

$$E_z = \frac{m_j}{e_j} \frac{\partial}{\partial t} V_{jz} - \frac{\dot{a}}{a} \cdot \frac{B_0(t)}{c \lambda} \cdot x^2.$$

Substitution Eq.(2.14) into the above equation gives

$$E_z = \frac{m_j}{e_j} \frac{\partial}{\partial t} V_{jz} - \frac{\dot{a}}{a^3} \cdot \frac{B_{00}}{c \lambda} \cdot x^2. \quad (2.27)'$$

From Eqs.(2.19) and (2.20), we obtain

$$V_{jz} = \frac{m_e}{m_j} \cdot \frac{c B_{00}}{4\pi e_j n_0 \lambda a}.$$

Partially differentiation both sides by time gives

$$\frac{\partial}{\partial t} V_{jz} = -\frac{m_e}{m_j} \cdot \frac{c B_{00} \dot{a}}{4\pi e_j n_0 \lambda a^2} \quad \left[= \frac{d}{dt} V_{jz} \right]$$

Substituting this into Eq.(2.27)', we can get the following expression for E_z :

$$E_z = -\frac{c B_{00} m_e}{4\pi e^2 n_0 \lambda} \cdot \frac{\dot{a}}{a^2} - \frac{B_{00}}{c \lambda} \cdot \frac{\dot{a}}{a^3} \cdot x^2. \quad (2.27)$$

2.5 Equation of Motion for a Test Particle

Here we consider the equations of motion for a test particle which moves in the electromagnetic fields given in the previous section. The relation between momentum \mathbf{P} and velocity \mathbf{V} of a test particle is given by

$$\mathbf{P}_j = m_j \Gamma_j \mathbf{V}_j$$

where Γ_j is

$$\Gamma_j = \frac{1}{\sqrt{1 - |\mathbf{V}_j|^2/c^2}}.$$

Eliminating \mathbf{V}_j from the above two equations,

$$\Gamma_j = \sqrt{1 + |\mathbf{P}_j|^2/(m_j c)^2}.$$

Therefore, we have

$$\mathbf{V}_j = \frac{\mathbf{P}_j}{m_j \sqrt{1 + |\mathbf{P}_j|^2/(m_j c)^2}} \quad (2.28)$$

The equation of motion for a charged particle is given as follows,

$$\dot{\mathbf{P}}_j = e_j \left(\mathbf{E} + \frac{\mathbf{V}_j}{c} \times \mathbf{B} \right). \quad (2.29)$$

Substituting Eq. (2.28) into (2.29), we have

$$\dot{\mathbf{P}}_j = e_j \left[\mathbf{E} + \frac{\mathbf{P}_j \times \mathbf{B}}{m_j c \sqrt{1 + |\mathbf{P}_j|^2/(m_j c)^2}} \right].$$

Now we split this into three components as follows,

$$\dot{P}_{jx} = e_j \left[E_x + \frac{P_{jy}B_z - P_{jz}B_y}{m_j c \sqrt{1 + |\mathbf{P}_j|^2/(m_j c)^2}} \right],$$

$$\dot{P}_{jy} = e_j \left[E_y + \frac{P_{jz}B_x - P_{jx}B_z}{m_j c \sqrt{1 + |\mathbf{P}_j|^2/(m_j c)^2}} \right],$$

$$\dot{P}_{jz} = e_j \left[E_z + \frac{P_{jx}B_y - P_{jy}B_x}{m_j c \sqrt{1 + |\mathbf{P}_j|^2/(m_j c)^2}} \right].$$

After substituting the electromagnetic fields in the previous section, we get the following equations;

$$\begin{aligned} \dot{P}_{jx} = e_j & \left[\left[-\frac{m_i V_a^2}{e \lambda a^3} + \frac{p_{0e}}{e \lambda a^{\gamma+1} n_0} \right] \cdot \frac{x}{\lambda} \right. \\ & \left. + \frac{1}{m_j c \sqrt{1 + |\mathbf{P}_j|^2/(m_j c)^2}} \cdot \left[P_{jy}B_z - P_{jz} \frac{B_{00}}{a^2} \cdot \frac{x}{\lambda} \right] \right], \end{aligned} \quad (2.30)$$

$$\dot{P}_{jy} = -\frac{e_j P_{jx} B_z}{m_j c \sqrt{1 + |\mathbf{P}_j|^2/(m_j c)^2}}, \quad (2.31)$$

$$\dot{P}_{jz} = e_j \left[-\frac{c B_{00} m_e}{4 \pi e^2 n_0 \lambda} \cdot \frac{\dot{a}}{a^2} - \frac{B_{00}}{c \lambda} \cdot \frac{\dot{a}}{a^3} \cdot x^2 + \frac{P_{jx} B_{00} x}{a^2 \lambda m_j c \sqrt{1 + |\mathbf{P}_j|^2/(m_j c)^2}} \right]. \quad (2.32)$$

2.6 Derivation of Charged Particle's Position x , y , z

Since momentum \mathbf{P}_j is represented as $\mathbf{P}_j = m_j \Gamma_j \mathbf{V}_j$, it is clear that

$$\dot{x}_j = \frac{P_{jx}}{m_j \Gamma_j}, \quad (2.33)$$

$$\dot{y}_j = \frac{P_{jy}}{m_j \Gamma_j}, \quad (2.34)$$

$$\dot{z}_j = \frac{P_{jz}}{m_j \Gamma_j}. \quad (2.35)$$

Therefore the position of a particle is given by integrating the above equations.

2.7 Derivation of Scale Factor $a(t)$

Since we have assumed $n_i = n_e$, the scale factor $a(t)$ is equal to $b(t)$. Therefore we derive $a(t)$ only.

Substituting $a(t) = b(t)$ into Eqs.(2.24) and (2.25), we get

$$\ddot{a} = -\frac{B_{00}^2}{4\pi m_e n_0 \lambda^2 a^2} + \frac{p_{0e}}{m_e n_0 \lambda^2 a^\gamma},$$

$$\ddot{b} = \frac{p_{0i}}{m_i n_0 \lambda^2 a^\gamma}.$$

Multiplying m_e in the above equation and m_i in the lower, respectively, and adding the two equations, we obtain

$$(m_e + m_i)\ddot{a} = -\frac{B_{00}^2}{4\pi n_0 \lambda^2 a^2} + \frac{p_{0e} + p_{0i}}{n_0 \lambda^2 a^\gamma},$$

which can be written as

$$\ddot{a} = -\frac{V_a^2}{\lambda^2 a^2} + \frac{C_s^2}{\lambda^2 a^\gamma}, \quad (2.36)$$

where

$$V_a^2 = \frac{B_{00}^2}{4\pi n_0 (m_e + m_i)}, \quad C_s^2 = \frac{p_{0e} + p_{0i}}{(m_e + m_i) n_0}.$$

2.8 Summary of Basic Equations

Here, we summarize the derived equations. We assume that particle density and pressure for protons are equal to ones for electrons, respectively. Therefore, we can represent $n_e = n_i = n_0$ and $p_{0e} = p_{0i} = p_0$. The equations of various quantities are summarized as follows:

$$\ddot{a} = -\frac{V_a^2}{\lambda^2 a^2} + \frac{C_s^2}{\lambda^2 a^\gamma}, \quad (2.37)$$

$$\dot{x}_j = \frac{P_{jx}}{m_j \Gamma_j}, \quad (2.38)$$

$$\dot{P}_{jx} = e_j \left[\left[-\frac{m_i V_a^2}{e \lambda a^3} + \frac{p_0}{e \lambda a^{\gamma+1} n_0} \right] \cdot \frac{x}{\lambda} + \frac{1}{m_j c \sqrt{1 + |\mathbf{P}_j|^2 / (m_j c)^2}} \cdot \left[P_{jy} B_z - P_{jz} \frac{B_{00}}{a^2} \cdot \frac{x}{\lambda} \right] \right], \quad (2.39)$$

$$\dot{y}_j = \frac{P_{jy}}{m_j \Gamma_j}, \quad (2.40)$$

$$\dot{P}_{jy} = -\frac{e_j P_{jx} B_z}{m_j c \sqrt{1 + |\mathbf{P}_j|^2 / (m_j c)^2}}, \quad (2.41)$$

$$\dot{z}_j = \frac{P_{jz}}{m_j \Gamma_j}, \quad (2.42)$$

$$\dot{P}_{jz} = e_j \left[-\frac{c B_{00} m_e}{4\pi e^2 n_0 \lambda} \cdot \frac{\dot{a}}{a^2} - \frac{B_{00}}{c \lambda} \cdot \frac{\dot{a}}{a^3} \cdot x^2 + \frac{P_{jx} B_{00} x}{a^2 \lambda m_j c \sqrt{1 + |\mathbf{P}_j|^2 / (m_j c)^2}} \right], \quad (2.43)$$

$$E_x = \left[-\frac{m_i V_a^2}{e \lambda a^3} + \frac{p_0}{e \lambda a^{\gamma+1} n_0} \right] \cdot \frac{x}{\lambda}, \quad (2.44)$$

$$E_z = -\frac{cB_{00}m_e}{4\pi e^2 n_0 \lambda} \cdot \frac{\dot{a}}{a^2} - \frac{B_{00}}{c\lambda} \cdot \frac{\dot{a}}{a^3} \cdot x^2, \quad (2.45)$$

$$B_y = \frac{B_{00}}{a^2} \cdot \frac{x}{\lambda}, \quad (2.46)$$

$$n_e = n_i = \frac{n_0}{a}. \quad (2.47)$$

And

$$V_a^2 = \frac{B_{00}^2}{4\pi n_0 (m_e + m_i)}, \quad (2.48)$$

$$C_s^2 = \frac{2p_0}{(m_e + m_i)n_0}, \quad (2.49)$$

$$\Gamma_j = \sqrt{1 + |\mathbf{P}_j|^2 / (m_j c)^2}. \quad (2.50)$$

3. OPERATIONS FOR SIMULATION OF THE EXPLOSIVE COALESCENCE

In this section, we will describe the method of numerical simulation and the normalization of physical quantities, and also determine their initial conditions for the differential equations.

3.1 Summary of Normalized Physical Quantities

If the derived equations are numerically treated in a computer, it is possible to occur an overflow error or an underflow error. Because some variables in the equations might have an enormous or nearly zero numbers (for example, $c = 3.0 \times 10^{10}$ cm/sec, $m_e = 9.1 \times 10^{-28}$ g). To avoid these numerical errors, every variables are used to be normalized.

Since $a(t)$ is a non-negative non-dimensional variable, it is not necessary to normalize it.

Now we define the normalized variables as follows.

$$\tilde{t} = \frac{t}{T}, \quad \tilde{x} = \frac{x}{\lambda}, \quad \tilde{P} = \frac{P}{m_j c}, \quad \tilde{E} = \frac{E}{m_j c^2 / (e\lambda)}, \quad \tilde{B} = \frac{B}{B_{00}}, \quad \tilde{n} = \frac{n}{n_0}.$$

Then, we can derive the following equations:

$$\dot{a} = \frac{da}{dt} = \frac{1}{T} \cdot \frac{da}{d\tilde{t}}, \quad \ddot{a} = \frac{d^2 a}{dt^2} = \frac{1}{T^2} \cdot \frac{d^2 a}{d\tilde{t}^2}, \quad \dot{P} = \frac{dP}{dt} = \frac{m_j c}{T} \cdot \frac{d^2 \tilde{P}}{d\tilde{t}^2}.$$

Therefore, Eqs. (2.37) ~ (2.47) without the suffix j for particle species can be normalized as follows,

$$\ddot{a} = -\frac{M_a^2}{a^2} + \frac{M_s^2}{a^\gamma}, \quad (3.1)$$

$$\dot{\tilde{x}} = \frac{\tilde{P}_x}{\sqrt{1 + |\tilde{\mathbf{P}}|^2}}, \quad (3.2)$$

$$\dot{\tilde{P}}_x = C_r \cdot \left[M_r \left[-\frac{M_{a1}^2}{a^3} + \frac{M_{s1}^2}{a^{\gamma+1}} \right] \cdot \tilde{x} + \frac{R_c}{\sqrt{1 + |\tilde{\mathbf{P}}|^2}} \cdot \left[\tilde{P}_y \tilde{B}_z - \tilde{P}_z \frac{\tilde{x}}{a^2} \right] \right], \quad (3.3)$$

$$\dot{\tilde{y}} = \frac{\tilde{P}_y}{\sqrt{1 + |\tilde{\mathbf{P}}|^2}}, \quad (3.4)$$

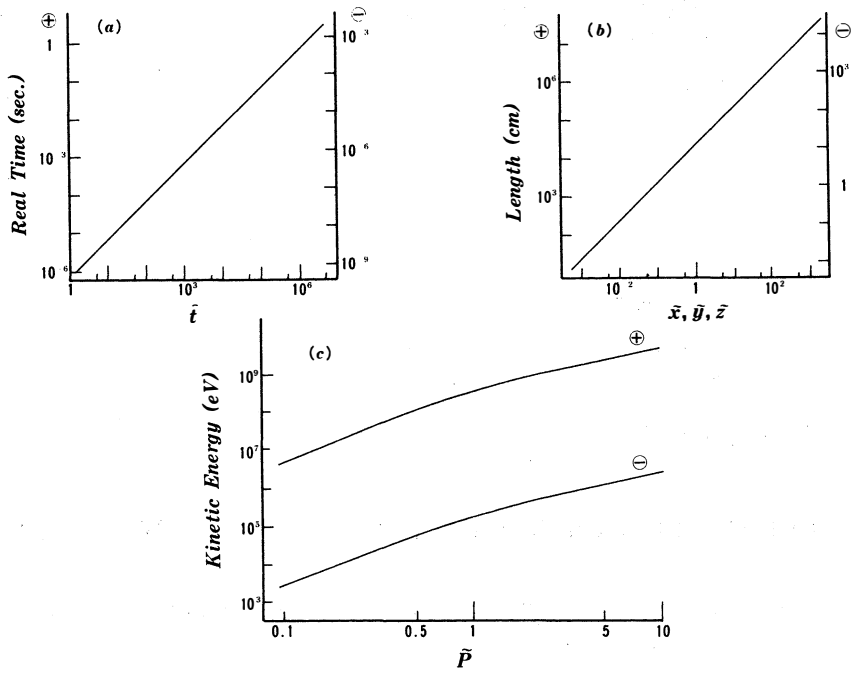


Fig.2. Relations between dimensional and non-dimensional quantities of (a) time, (b) length, (c) kinetic energy.

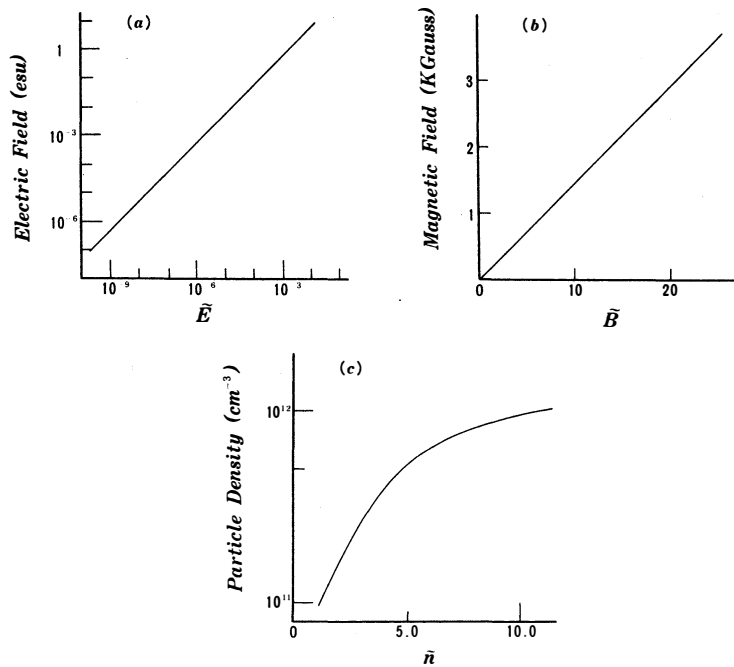


Fig.3. Relations between dimensional and non-dimensional quantities of (a) electric field, (b) magnetic field, (c) particle density.

$$\dot{\tilde{P}}_y = -C_r \cdot \frac{R_c}{\sqrt{1+|\tilde{\mathbf{P}}|^2}} \cdot \tilde{P}_x \tilde{B}_z, \quad (3.5)$$

$$\dot{\tilde{z}} = \frac{\tilde{P}_z}{\sqrt{1+|\tilde{\mathbf{P}}|^2}}, \quad (3.6)$$

$$\dot{\tilde{P}}_z = C_r \cdot \left[-\frac{R_c}{R_p^2} \cdot \frac{\dot{a}}{a^2} - R_c \cdot \frac{\dot{a}}{a^3} \cdot \tilde{x}^2 + \frac{R_c}{\sqrt{1+|\tilde{\mathbf{P}}|^2}} \cdot \tilde{P}_x \cdot \frac{\tilde{x}}{a^2} \right], \quad (3.7)$$

$$\tilde{E}_x = M_r \cdot \left[-\frac{M_{a1}^2}{a^3} + \frac{M_{s1}^2}{a^{\gamma+1}} \right] \cdot \tilde{x} \quad (= \tilde{E}_0 \cdot \tilde{x}), \quad (3.8)$$

$$\tilde{E}_z = -\frac{R_c}{R_p^2} \cdot \frac{\dot{a}}{a^2} - R_c \cdot \frac{\dot{a}}{a^3} \cdot \tilde{x}^2 \quad (= \tilde{E}_{z0} + \tilde{E}_{z1} \cdot \tilde{x}^2), \quad (3.9)$$

$$\tilde{B}_y = \frac{\tilde{x}}{a^2} \quad (= \tilde{B}_0 \cdot \tilde{x}). \quad (3.10)$$

$$\tilde{n} = \frac{1}{a}. \quad (3.11)$$

Other normalized physical quantities are summarized as follows,

$$M_a^2 = \frac{V_a^2}{c^2}, \quad (3.12)$$

$$M_s^2 = \frac{C_s^2}{c^2}, \quad (3.13)$$

$$M_{a1}^2 = \frac{V_a^2}{c^2}, \quad (3.14)$$

$$M_{s1}^2 = \frac{p_0}{m_p n_0 c^2}, \quad (3.15)$$

$$R_c = \omega_{cj} T, \quad (3.16)$$

$$R_p^2 = \omega_{pe}^2 T^2, \quad (3.17)$$

$$C_r = \frac{e_j}{e}, \quad (3.18)$$

$$M_r = \frac{m_i}{m_j}, \quad (3.19)$$

$$\gamma = 1 + \frac{2}{f}, \quad (3.20)$$

where

$$\omega_{cj} = \frac{eB_{00}}{m_j c}, \quad (3.21)$$

$$\omega_{pe}^2 = \frac{4\pi n_0 e^2}{m_e}. \quad (3.22)$$

To solve the coupled nonlinear differential equations, we used ODAM (Adams method to solve a simultaneous first differential equations). To use this method, several quantities are defined as follows,

$$y_1 = a, \quad y_2 = \dot{a}, \quad y_3 = \tilde{x}, \quad y_4 = \tilde{P}_x,$$

$$y_5 = \tilde{y}, \quad y_6 = \tilde{P}_y, \quad y_7 = \tilde{z}, \quad y_8 = \tilde{P}_z.$$

And Eqs. (3.1) ~ (3.7) are transformed into the following eight simultaneous first order differential equations;

$$\dot{y}_1 = y_2, \quad (3.23)$$

$$\dot{y}_2 = -\frac{M_a^2}{y_1^2} + \frac{M_s^2}{y_1^\gamma}, \quad (3.24)$$

$$\dot{y}_3 = \frac{y_4}{\sqrt{1+|\tilde{P}|^2}}, \quad (3.25)$$

$$\dot{y}_4 = C_r \cdot \left[M_r \cdot \left[-\frac{M_{a1}^2}{y_1^3} + \frac{M_{s1}^2}{y_1^{\gamma+1}} \right] \cdot y_3 + \frac{R_c}{\sqrt{1+|\tilde{P}|^2}} \cdot \left[y_6 \tilde{B}_z - y_8 \frac{y_3}{y_1^2} \right] \right], \quad (3.26)$$

$$\dot{y}_5 = \frac{y_6}{\sqrt{1+|\tilde{P}|^2}}, \quad (3.27)$$

$$\dot{y}_6 = C_r \frac{R_c}{\sqrt{1+|\tilde{P}|^2}} \cdot y_4 \tilde{B}_z, \quad (3.28)$$

$$\dot{y}_7 = \frac{y_8}{\sqrt{1+|\tilde{P}|^2}}, \quad (3.29)$$

$$\dot{y}_8 = C_r \cdot \left[-\frac{R_c}{R_p^2} \cdot \frac{y_2}{y_1^2} - R_c \cdot \frac{y_2}{y_1^3} \cdot y_3^2 + \frac{R_c}{\sqrt{1+|\tilde{P}|^2}} \cdot y_4 \cdot \frac{y_3}{y_1^2} \right], \quad (3.30)$$

here

$$|\tilde{P}|^2 = y_4^2 + y_6^2 + y_8^2.$$

3.2 Determination of Initial Conditions

Initial values of physical quantities are necessary to solve the above simultaneous equations. In this section we will define various normalized physical quantities in the basic equations and determine the initial values.

3.2.1. DETERMINATION OF PARAMETERS

Before determination of initial values, we have to set the values of parameters involved in the basic equations.

For simulations, we use magnetic field and density of the typical solar flare region as

$$B_{00} = 145 \text{ Gauss},$$

$$n_0 = 10^{11}/\text{cm}^3.$$

In Eq. (3.1) the first term of right hand side corresponds to the $\mathbf{J} \times \mathbf{B}$ term and drives the magnetic collapse. While the second term corresponds to the pressure gradient term and may eventually be able to balance with the magnetic compression term when $\gamma = 3$. The condition $\gamma = 3$ which we will use here means that the current loop coalescence occurs in nearly one-dimensional fashion so that the degree of freedom of the system becomes unity. The plasma β

value ($\beta = C_s^2/V_a^2$) is varied from 0.1 to 1.0. From the above quantities, we can calculate following quantities;

$$\begin{aligned}\omega_{pe}^2 &= \frac{4\pi n_0 e^2}{m_e}, \\ \omega_{cj} &= \frac{eB_{00}}{m_j c}, \\ p_0 &= \frac{B_{00}^2}{8\pi} \cdot \beta, \\ T &= \frac{1}{\omega_{cj}} = \frac{m_j c}{eB_{00}}, \\ \lambda &= cT = \frac{m_j c^2}{eB_{00}}, \\ V_a^2 &= \frac{B_{00}^2}{4\pi n_0 (m_e + m_i)} \approx \frac{B_{00}^2}{4\pi n_0 m_i}, \\ C_s^2 &= \frac{2p_0}{(m_e + m_i)n_0} \approx \frac{2p_0}{m_i n_0}.\end{aligned}$$

Here, we note that standard values of time T , length λ , and momentum $m_j c$ are changed by the species of particles. (For electric field, $m_j c^2 / (e\lambda) = B_{00}$.) Fig.2 and 3 show the relation of non-dimensional quantities and dimensional quantities, based on the above values.

3.2.2. DETERMINATION OF THE INITIAL VALUES

Because the basic equations numerically solved are eight-dimensions, we need eight initial values. For location and momentum of a charged particle, they are varied in the following ranges.

$$\tilde{x}, \tilde{y}, \tilde{z} = 0.0 \sim 4.0$$

$$\tilde{P}_x, \tilde{P}_y, \tilde{P}_z = \pm 10^{-6} \sim 10^{-4}$$

Next, we discuss about the determination of initial values of a and \dot{a} . Eq.(3.1) can be rewritten as follows,

$$\ddot{a} = -\frac{\partial}{\partial a} V(a), \quad (3.31)$$

here $V(a)$ is the effective (Sagdeev) potential, which is given by

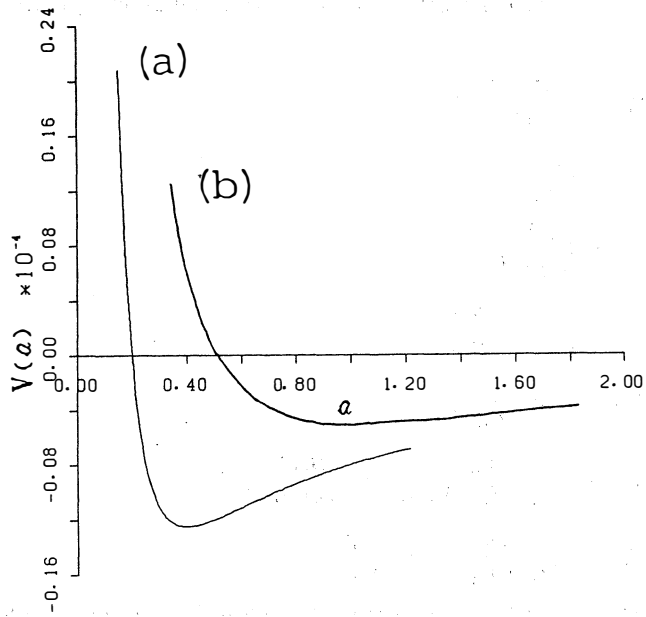
$$V(a) = -\frac{M_a^2}{a} + \frac{M_s^2}{2a^2}. \quad (3.32)$$

The graph of the effective potential is shown in Fig.4. The minimum value V_{\min} is obtained from the condition of $\partial V(a)/\partial a = 0$.

$$V_{\min} = -\frac{M_a^4}{2M_s^2} \quad \left[a = \frac{M_s^2}{M_a^2} \right]$$

If plasma β value varies, the shape of graph is changed by it as shown in Fig.4. If the plasma β becomes smaller, the shorter and deeper the potential bottom is. So, when the initial condition of a is close to V_{\min} , we have oscillational behavior of a near the potential minimum.

We assume that the initial values of a and \dot{a} are a_s and \dot{a}_s , respectively. From the rule of


 Fig.4. Effective potential $V(a)$: (a) $\beta = 0.4$, (b) $\beta = 1.0$.

energy conservation, we obtain

$$\frac{1}{2}m_j(\dot{a}_s)^2 = -m_j \int_{a_s}^{a_e} \ddot{a} da, \quad (3.33)$$

where a_e is the edge of oscillation in a -axis. We regard Eq. (3.33) as a second order equation for a_e , and arranging it, we get

$$\left[(\dot{a}_s)^2 - 2 \cdot \frac{M_a^2}{a_s} + \frac{M_s^2}{a_s^2} \right] \cdot a_e^2 + 2M_a^2 a_e - M_s^2 = 0.$$

From the conditions of existence of solutions, we obtain

$$|\dot{a}_s| < \sqrt{2M_a^2/a_s - M_s^2/a_s^2} \quad (\text{note: } a_s > \frac{\beta}{2}) \quad (3.34)$$

If the start point a_s is at the bottom of the potential ($a_s = \beta$), Eq. (3.34) is rewritten as follows;

$$|\dot{a}_s| < \sqrt{(M_a^2)^2/M_s^2} = \sqrt{M_a^2/\beta}. \quad (3.35)$$

We determine the initial value of \dot{a} from Eq. (3.35), as the initial value of a is equal to the plasma β value.

4. SIMULATION RESULTS

In this section, we will show the simulation results obtained by means of the basic equations derived in the previous section. At first in our simulations, we determine β , \vec{B}_z , and the eight initial values of simultaneous differential equations as follows;

$$\beta = 0.4, \quad \tilde{B}_z = 1.0,$$

$$a = \beta, \quad \dot{a} = -\beta \times 10^{-2}, \quad (\dot{a}/a = -10^{-2})$$

$$\tilde{x} = 1.0, \quad \tilde{y} = \tilde{z} = 0.0,$$

$$\tilde{P}_x = \tilde{P}_y = \tilde{P}_z = 10^{-6}.$$

Next we will change four parameters β , \tilde{B}_z , \dot{a}/a , and \tilde{x} , which have important effects on the particle acceleration.

4.1 Electromagnetic Field and Density during Current Loop Coalescence

In this section, we will show how the electromagnetic fields, density and coalescence period can change depending on β and \dot{a}/a during the current loop coalescence. These physical quantities have the periodic characteristics in time. Then, in Figs.5~7, both of maximum and minimum values for every quantity are dotted and are connected with each other.

Fig.5 shows the parameter dependence of \tilde{B}_0 and \tilde{n} . As shown in Figs.5(a) and (c), if β becomes smaller, both values of \tilde{B}_0 and \tilde{n} become larger. This means that for the low β plasma strong plasma compression can occur by the Lorentz force (magnetic collapse) during the current loop coalescence. And, as β is large, they are almost constant. The dependence on \dot{a}/a shown in Figs.5(b) and (d) shows that both \tilde{B}_0 and \tilde{n} increase with increment of \dot{a}/a . This means

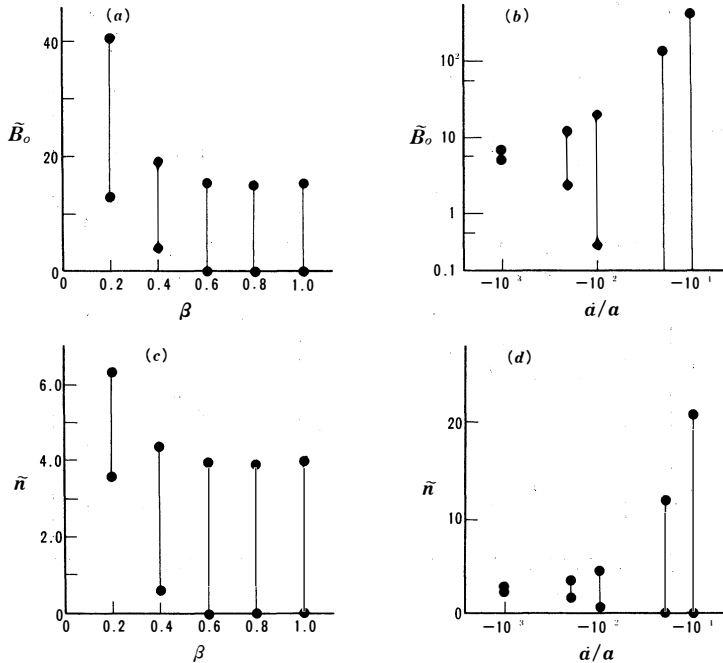


Fig.5. \tilde{B}_0 depends on (a) β , (b) \dot{a}/a . \tilde{n} depends on (c) β , (d) \dot{a}/a .

that if the initial colliding velocity ($\propto \dot{a}/a$) becomes large, strong magnetic collapse can occur with strong density accumulation.

Fig.6 shows the parameter dependence of \bar{x} -component E_0 of electric field. Fig.6(b) shows that \dot{a}/a approaches to -0.1 , the maximum value of \tilde{E}_0 suddenly can become large. This effect may be important for the high energy particle production. For \bar{z} -components \tilde{E}_{z0} and \tilde{E}_{z1} as shown in Fig.7, the coefficient \tilde{E}_{z1} proportional to \bar{x} is much larger than \tilde{E}_{z0} . This means that the amount of acceleration in \bar{z} -direction depends on the location of particles in \bar{x} -direction.

Fig.8 shows the parameter dependence of the period on β and \dot{a}/a . When β as well as \dot{a}/a is large, the period is long. Because the bottom of effective potential $V(a)$ becomes shallow and flat.

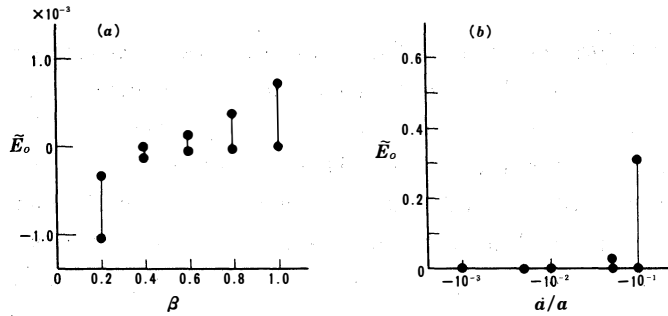


Fig.6. \tilde{E}_0 depends on (a) β , (b) \dot{a}/a .

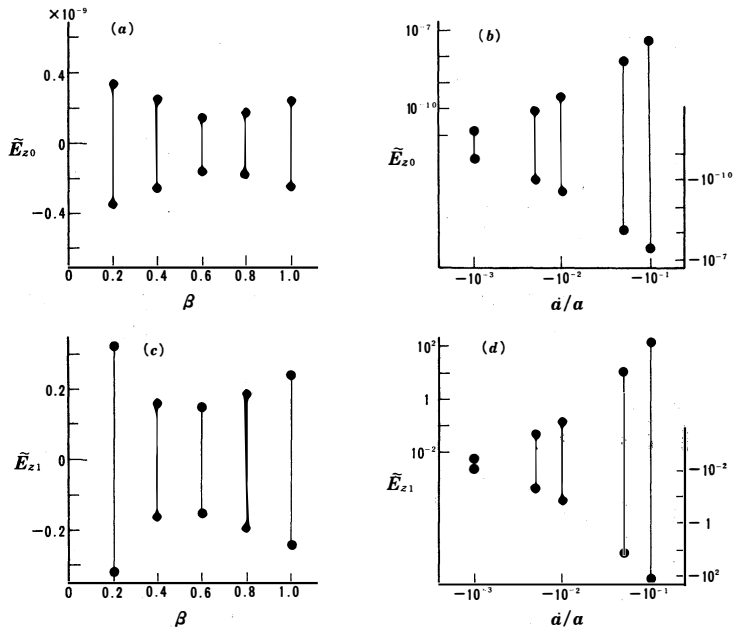


Fig.7. Electric field components depend on β and \dot{a}/a .

4.2 Particle Acceleration to Relativistic Energies

We will show that both electrons and protons can be periodically accelerated to relativistic energies during the current loop coalescence. Figs.9~12 show the parameter dependences of maximum value \tilde{P}_{max} of momentum and its components \tilde{P}_x , \tilde{P}_y , and \tilde{P}_z under several conditions.

Fig.9(a) shows β dependence of \tilde{P}_{max} which has a peak around $\beta \simeq 0.4$. The peak value is 2.4, which corresponds to about 2 GeV for protons, about 1.22 MeV for electrons. Since the bottom of the effective potential $V(a)$ becomes shallower with increasing β , particle's oscillatory behavior is transformed into non-oscillatory behavior. In Fig.9(a), non-oscillatory behavior occurs at $\beta > 0.5$.

Fig.9(b) shows \tilde{B}_z dependence. When $\tilde{B}_z = 0$, charged particles are hardly accelerated. But

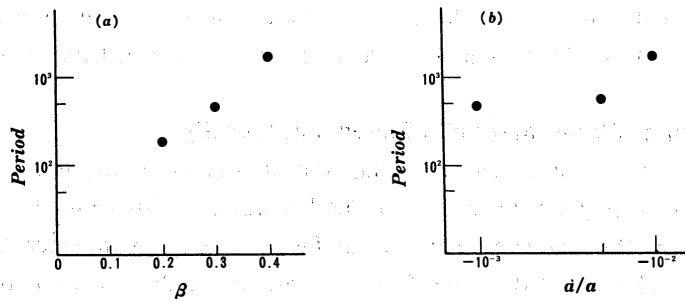


Fig.8. Periodic time depends on (a) β , (b) \dot{a}/a .

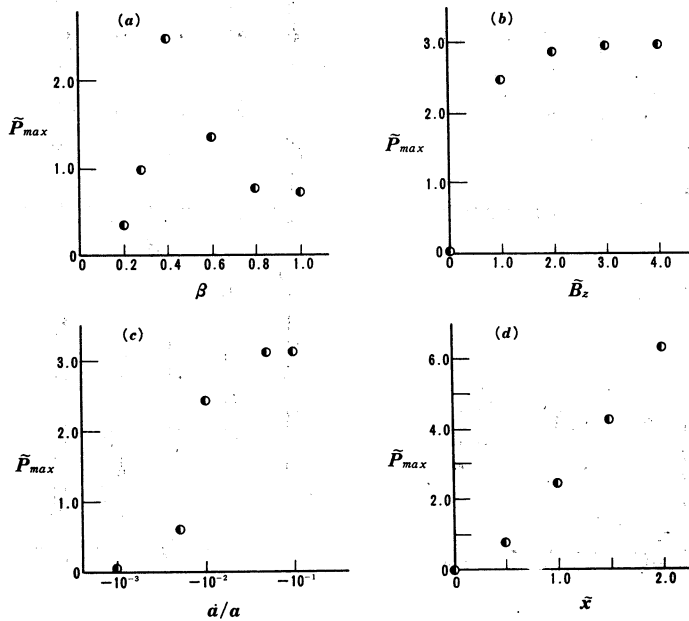


Fig.9. \tilde{P}_{max} depends on (a) β , (b) \tilde{B}_z , (c) \dot{a}/a , (d) \tilde{x} .

when \tilde{B}_z is beyond 1.0 (=145 Gauss), their kinetic energies are larger than rest-mass energies and seem to saturate. Therefore, the relativistic particle acceleration needs the existence of \tilde{B}_z essentially.

Fig.9(c) shows the dependence on \dot{a}/a . When $|\dot{a}/a|$ increases, \tilde{P}_{\max} increases. The explosive coalescence of plasma current loops is also important to get the relativistic energies for both electrons and protons.

Fig.9(d) shows the dependence on the initial particle location \tilde{x} . \tilde{P}_{\max} increases linearly with \tilde{x} . Particles located far from the center of current loop coalescence, can be well accelerated.

Figs.10(a) ~ (d) show the various parameter dependence of \tilde{x} -component \tilde{P}_x . As seen in Fig.10, the acceleration to \tilde{x} -direction is weak. (Here, for protons, O for electrons.)

Figs.11 and 12 show the parameter dependence of \tilde{P}_y and \tilde{P}_z , respectively. From these graphs, it is clear that protons and electrons can be accelerated to the opposite direction each other. \tilde{P}_y and \tilde{P}_z are 10 to 100 time as large as \tilde{P}_x after the current loop coalescence.

4.3 Time Evolution of Electromagnetic Fields and Density

The time evolution of electromagnetic fields and density is shown as a typical example, using standard values as they are determined at the beginning of this chapter.

Figs.13 ~ 15 show the time evolution of scale factor, electric field, magnetic field, and density. The oscillatory behavior of the scale factor a leads to similar oscillations in other physical

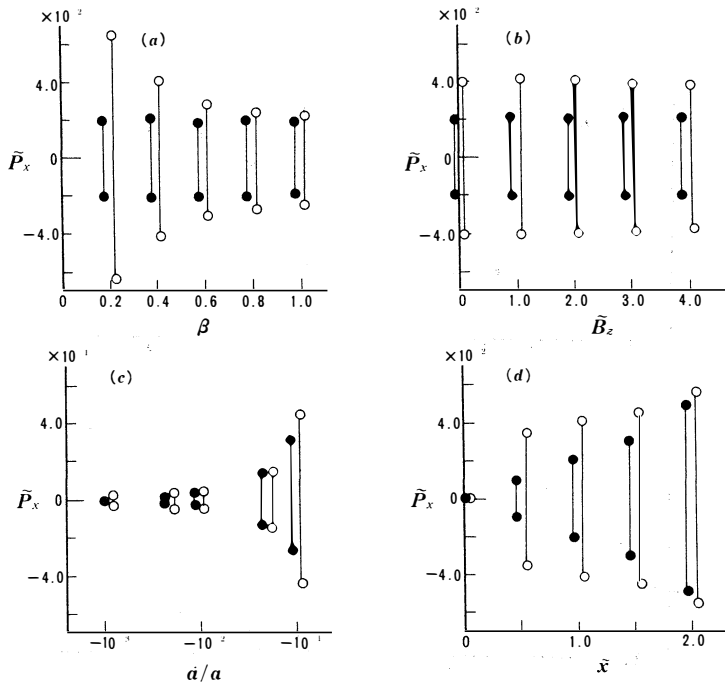


Fig.10. \tilde{P}_x depends on (a) β , (b) \tilde{B}_z , (c) \dot{a}/a , (d) \tilde{x} .

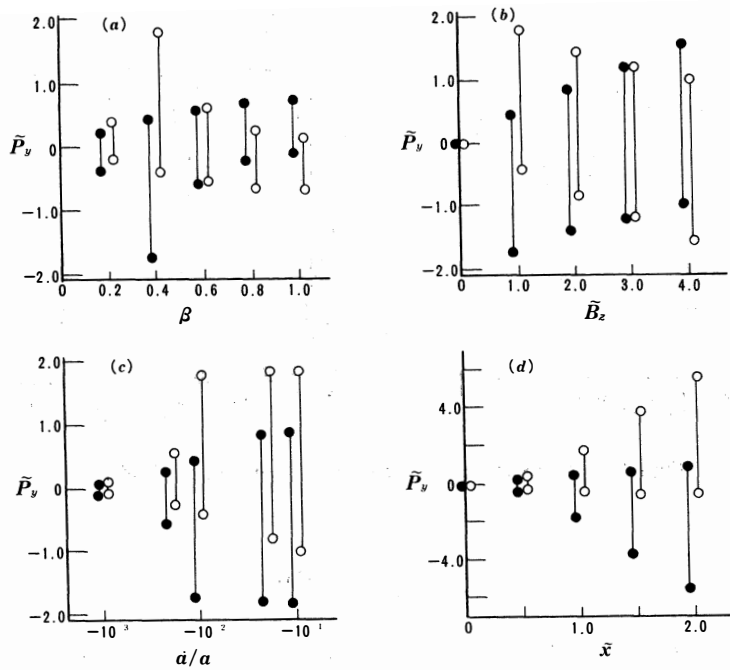


Fig.11. \tilde{P}_y depends on (a) β , (b) \tilde{B}_z , (c) \tilde{a}/a , (d) \tilde{x} .

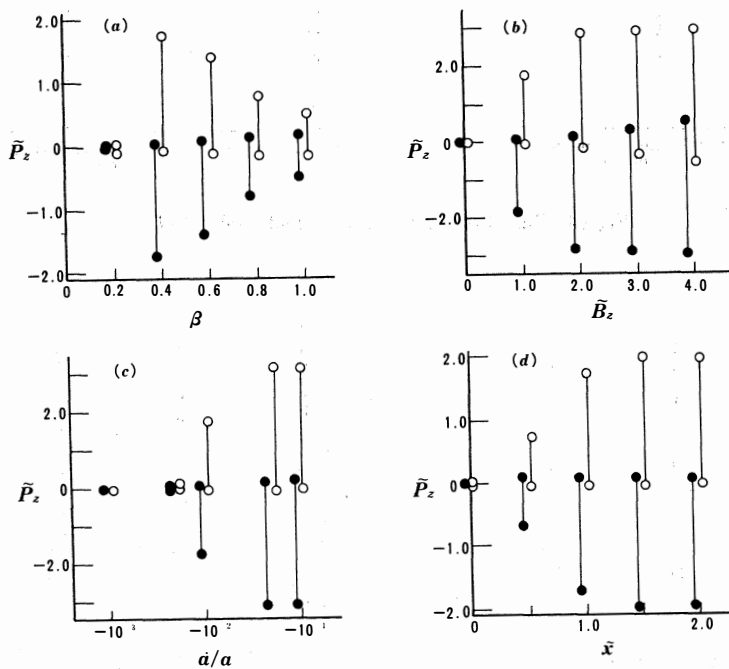


Fig.12. \tilde{P}_z depends on (a) β , (b) \tilde{B}_z , (c) \tilde{a}/a , (d) \tilde{x} .

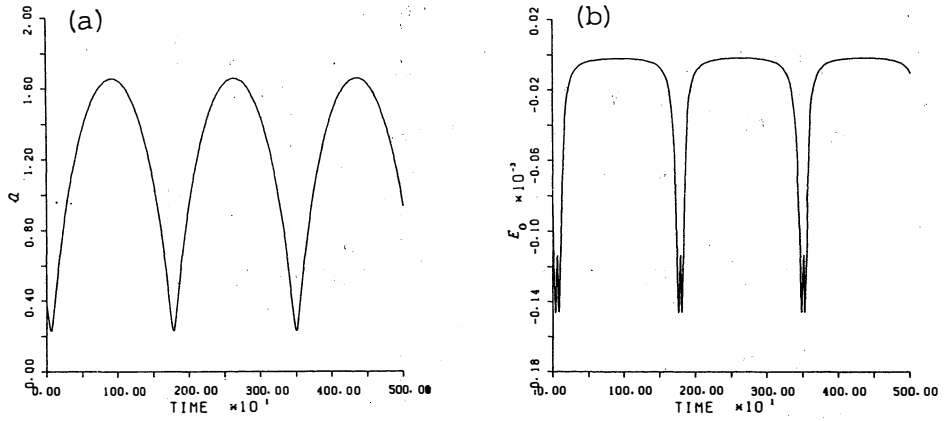


Fig.13. Time history of (a) scale factor a , (b) electric field \bar{E}_0 .

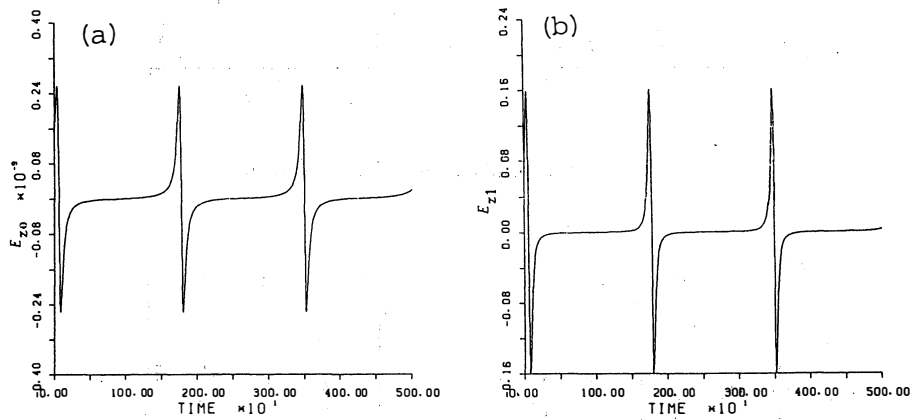


Fig.14. Time history of electric field; (a) \bar{E}_{z0} , (b) \bar{E}_{z1} .

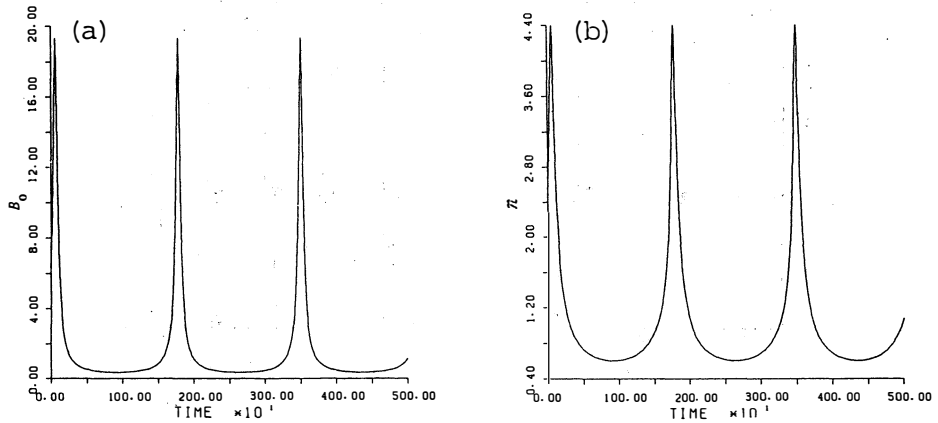


Fig.15. Time history of (a) magnetic field \bar{B}_0 , (b) particle density \bar{n} .

quantities. The period of a is about 1.7×10^3 , which corresponds to about 1.2 msec for protons, about $0.68 \mu\text{sec}$ for electrons. Other physical quantities have the same period. If β becomes smaller, double-peak structure (Fig.13(b)) on \tilde{E}_0 which occurs during the magnetic collapse phase disappears and \tilde{E}_0 changes like a sine wave.

4.4 Time Evolution of Momentum of Charged Particles

In this section, we will show the momentum and the orbit of proton when \tilde{B}_z and \tilde{x} are 4.0 and 1.0, respectively.

As seen in Fig.16(a), the momentum \tilde{P}_x varies with a very small time scale compared with \tilde{P}_y and \tilde{P}_z (see Figs.16(b) and Fig.17(a)). Furthermore, \tilde{P}_x has a high periodic behavior which corresponds to the period of the scale factor a . Fig.17(b) shows the time evolution of total momentum of proton. Fig.18 shows the orbit of proton which moves from large z to small z . (Many symbols in the orbit mean the time intervals. One interval is about $180 \mu\text{sec}$.)

Figs.19~21 show the behavior of proton when $\tilde{B}_z = 1.0$ and $\tilde{x} = 0.0$. This is an example that a proton is hardly accelerated. Indeed, in $\tilde{x}-\tilde{y}$ plane, the proton shows Larmor motion

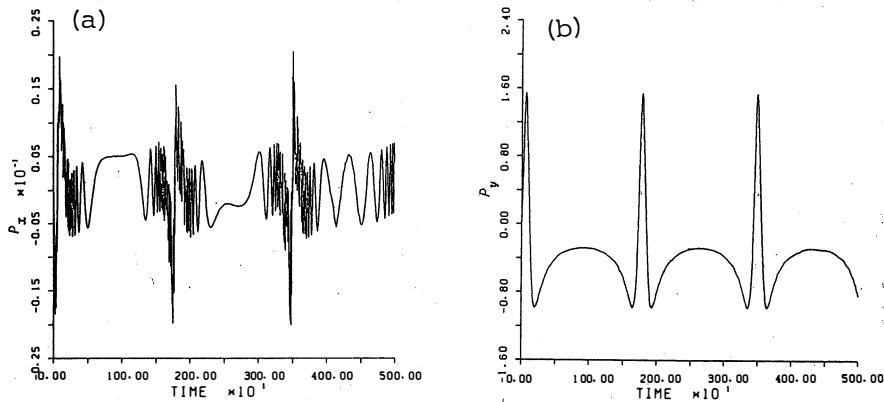


Fig.16. Time history of momentum; (a) \tilde{P}_x , (b) \tilde{P}_y .

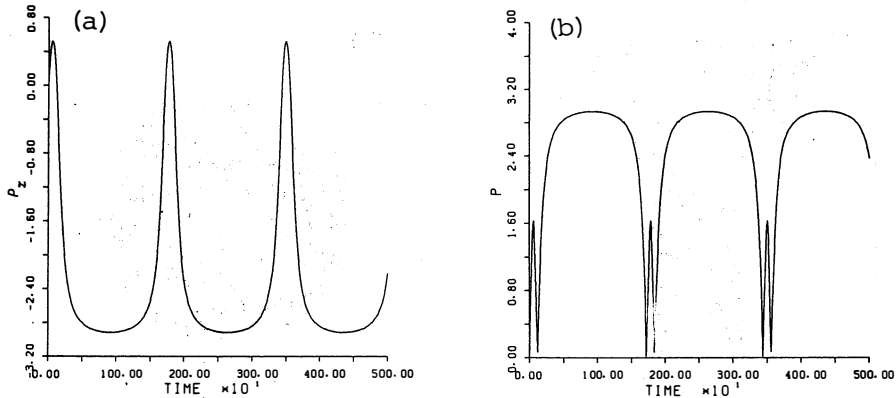


Fig.17. Time history of momentum; (a) \tilde{P}_z , (b) \tilde{P} .

around \tilde{B}_z . As seen in Fig.19(b), the change of total momentum during magnetic collapse is very small. Fig.20(a) and (b) show the orbit of the proton in x - y plane and y - z plane, respectively. Fig.21 shows its 3-D orbit. Figs.22 ~ 24 show the behavior of electron when $\tilde{B}_z = 1.0$ and $\tilde{x} = 1.5$. In \tilde{x} -direction, the electron behaves with the same manner of proton, because of the coalescence direction. But in \tilde{y} and \tilde{z} -directions (Figs.22(b), 23(a)), the electron can be accelerated in opposite directions compared with protons (see Figs.16(b), 17(a)). Fig.24 shows orbit of the electron which moves from small z to large z . The oscillatory acceleration period of the electron is the same with one of the scale factor a . Therefore we

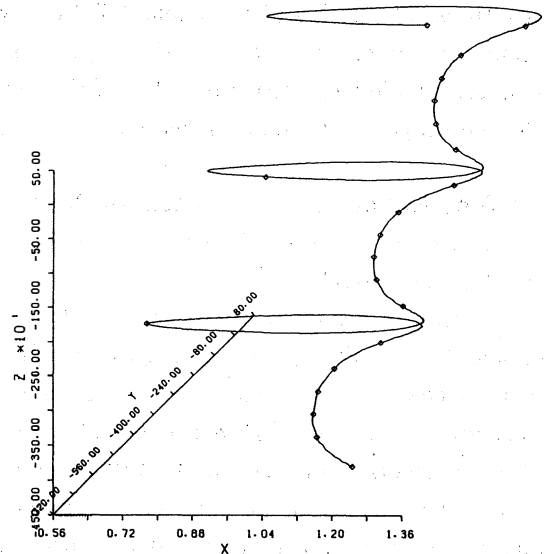


Fig.18. 3-D representation of proton's orbit.

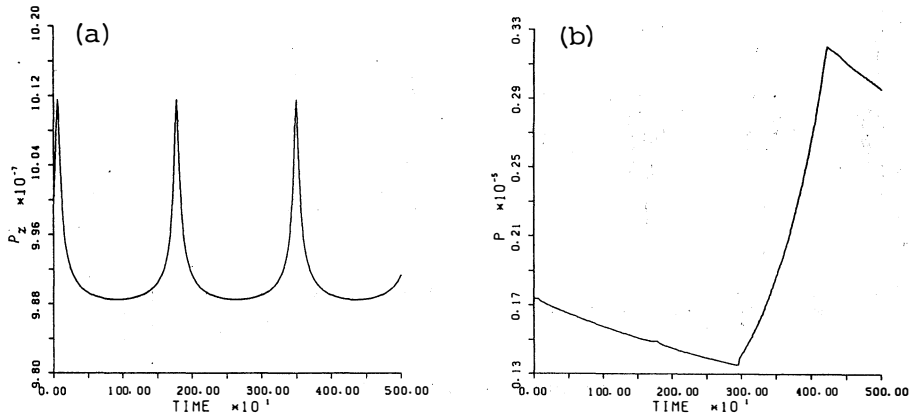


Fig.19. Time history of momentum; (a) \tilde{P}_x , (b) \tilde{P}_y .

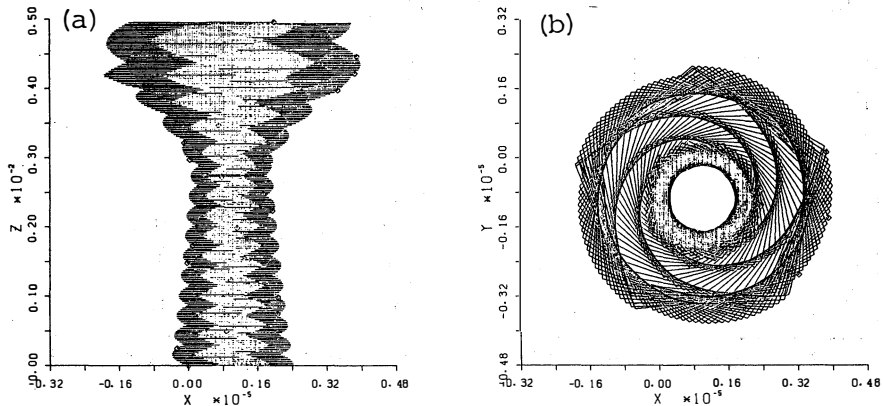


Fig.20. Proton's orbit in (a) \tilde{x} - \tilde{z} plane, (b) \tilde{x} - \tilde{y} plane.

may conclude that both electrons and protons can be quasi-periodically accelerated to relativistic energies during current loop coalescence.

5. SUMMARY AND DISCUSSION

In this paper, we investigated the explosive acceleration of charged particles (protons and electrons), using the plasma current loop coalescence model. We found that both electrons and protons can be quasi-periodically accelerated to the relativistic energies under several conditions. The important parameters for relativistic particle acceleration are (1) the plasma β ratio, (2) the magnetic field along the

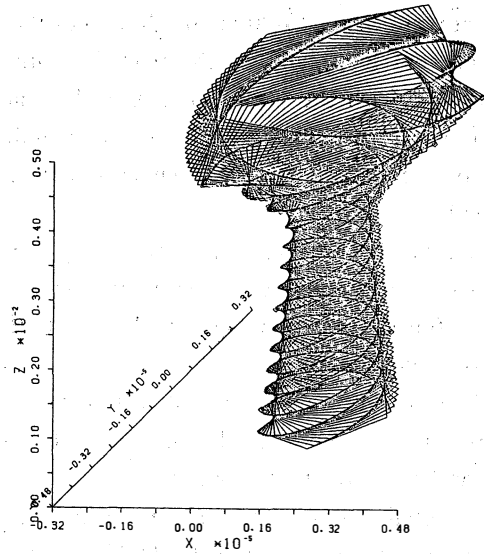


Fig.21. 3-D representation of proton's orbit.

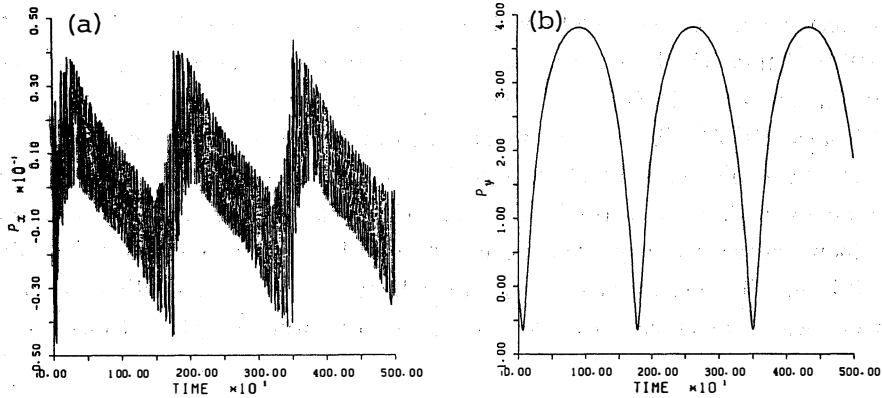


Fig.22. Time history of momentum; (a) \bar{P}_x , (b) \bar{P}_y .

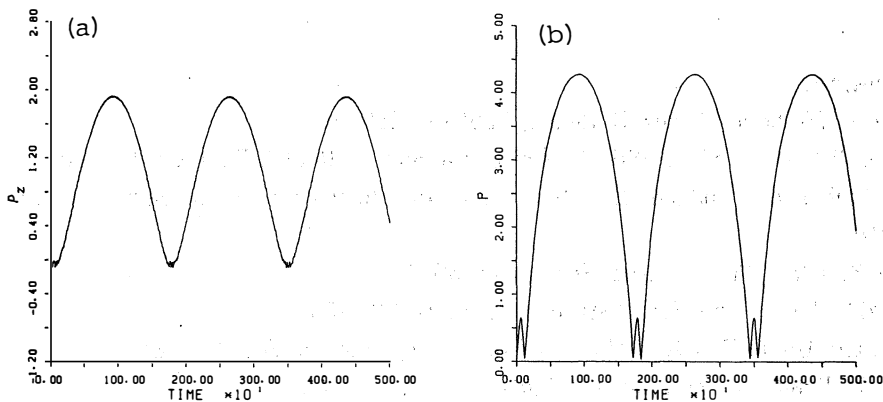


Fig.23. Time history of momentum; (a) \bar{P}_z , (b) \bar{P} .

two current loops, (3) high colliding velocity of the current loops and (4) the particle's initial location \bar{x} from the center of loop coalescence. Both electrons and protons can be simultaneously accelerated within much less than one second.

Recent observations for high energy particle acceleration during the impulsive phase in solar flares are summarized by de Jager (1989)¹² as follows:

- (1) The acceleration times of electrons and protons to energies of some tens of MeV can be shorter than ~ 2 sec.
- (2) Although MeV protons are accelerated nearly simultaneously with MeV electrons, observations with high time resolution show that the ionic emission can occur one to two seconds later.

- (3) Primary electrons are accelerated to energies of roughly ~ 100 MeV.

De Jager (1989)¹² explained these observations by the explosive current loop coalescence model proposed by Tajima et al. (1982,⁶ 1987)⁸ (see for review of the current loop coalescence model; Sakai and Ohsawa, 1987)¹⁰. The electron acceleration up to the observed energies (~ 100 MeV) is possible by the explosive current loop coalescence, if many current loop coalescence can occur successively within one second. Quasi-periodic relativistic electron acceleration during the current loop coalescence may cause observed short-lived micro-wave bursts¹³ with lifetimes down to ~ 0.1 sec. The quasi-periodic magnetic collapse can produce multiple strong fast magnetosonic shock wave,¹⁴ which can also produce high energy protons and electrons.¹⁰

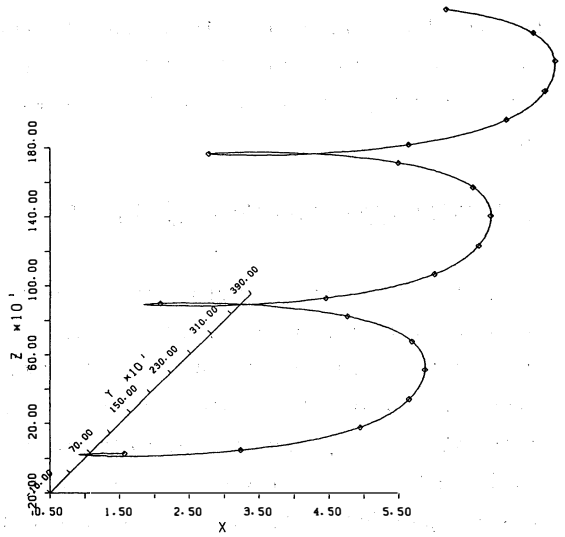


Fig.24. 3-D representation of electron's orbit.

Acknowledgement

We acknowledge for use of Computer Center, Toyama University.

References

1. Svestka, 1976, Solar Flares, D. Reidel, Publ. Co, Holland.
Sturrock, P.A. et al. eds. 1986, Physics of the Sun, D. Reidel. Publ. Co, Holland.
2. Kundu, M.R. and Woodgate, B. 1986, Energetic Phenomena on the Sun, NASA Conf. Publ., No.2439.
3. Tanaka, K. 1987, Publ. Astron. Soc. Japan. 39, 1.
4. Chupp, E.L. 1984, Ann. Rev. Astron. Astrophys. 22, 359.
5. Gold, T. and Hoyle, F. 1960, Monthly Notices Roy. Astron. Soc. 120, 89.
6. Tajima, T., Brunel, F., and Sakai, J. 1982, Ap. J. 245, L45.
7. Tajima, T. and Sakai, J. 1989a, Sov. J. Plasma Phys. in press

8. Tajima, T. and Sakai, J. 1989b, Sov. J. Plasma Phys. in press
9. Tajima, T., Sakai, J.-I., Nakajima, H., Kosugi, T., Brunel, F., and Kundu, M.R. 1987, Ap. J. 321, 1031.
10. Sakai, J.-I., and Ohsawa, Y. 1987, Space Sci. Rev., 46, 113.
11. Sakai, J. and Tajima, T. 1986, Proc. Joint Varenna-Abastumani International School and Workshop on Plasma Astrophysics, ESA SP-251, p.77.
12. De Jager, C. 1989, Advances in Space Research, in press
13. De Jager, C., Kuypers, J., Correia, E. and Kaufmann, P. 1987, Solar Phys. 110, 317.
14. Sakai, J. 1989, in preparation

(Received October, 31 1988)